ChemComm

COMMUNICATION

View Article Online
View Journal | View Issue

Cite this: *Chem. Commun.*, 2022, **58**, 8218

Received 16th May 2022,
Accepted 24th June 2022

DOI: 10.1039/d2cc02777a

rsc.li/chemcomm

Water vapour induced reversible switching between a 1-D coordination polymer and a 0-D aqua complex†

Min Deng,‡[a] Soumya Mukherjee, ‡[b] Yu-Jie Liang,[a] Xiao-Dan Fang,[a] Ai-Xin Zhu*[a] and Michael J. Zaworotko *[b]

[Zn(3-tba)$_2$], 1, a 1-D coordination polymer synthesised as 1 DMA, 1α, transformed to a nonporous form, 1β, upon activation. 1β underwent further transformation to the dimeric complex [Zn(3-tba)$_2$(H$_2$O)$_2$], 2, above 40% RH. The reverse transformations, 2 to 1β and 1β to 1α, were accomplished by heating and exposure to DMA, respectively, and were single-crystal-to-single-crystal phase changes. Single crystal X-ray diffraction revealed that the second transformation resulted from Zn–carboxylate bond breakage and concomitant coordination of water molecules. Other solvent molecules did not induce a phase change.

Metal–organic materials (MOMs),[1] especially porous MOMs such as metal–organic frameworks (MOFs)[2] and porous coordination polymers (PCPs),[3] have received considerable attention with respect to their gas and vapour adsorption properties.[4] Whereas >100 000 coordination networks have been deposited in the MOF subset of the Cambridge Structural Database (CSD),[5] only a small proportion, <100, are known to exhibit type F-IV isotherms with reversible transformations between nonporous (closed) and porous (open) phases.[6] Such stepped isotherms are of topical interest because their "switching" between closed and open phases can result in relatively high uptake capacity and, perhaps counter-intuitively, stronger separation selectivity than rigid porous materials with similar pore size.[7,8] Indeed, benchmark binding to C_2H_2 has been observed for a switching sorbent through an induced-fit mechanism reminiscent of enzyme–substrate binding.[9]

Single-crystal-to-single-crystal (SCSC) transformations in switching sorbents can provide insight into structure–property relationships through single-crystal X-ray diffraction (SCXRD).[10] SCSC transformations can typically be induced by external stimuli, *e.g.* gas/vapour uptake and/or removal,[11,12] temperature change,[13] pH change,[14] light[15] and cation or anion exchange.[16,17] Water vapour sorption is of particular relevance as it can bind with open metal centres[18,19] or physisorb, thereby being relevant to applications such as atmospheric water harvesting and dehumidification. Most MOMs exhibit type F-IV water vapour isotherms that result from pore filling (capillary condensation, Table S6 in ESI†).[20] Our literature survey revealed only 12 MOMs (Table S6, ESI†) that exhibit a type F-IV stepped isotherm caused by water-induced structural changes and, to our knowledge, water-induced 1D → 0D SCSC structural phase changes with a single-step are unstudied. Such transformations have the potential to exhibit high selectivity for water over alcohols. Indeed, some examples display selective water uptake over alcohols attributed to structural transformations.[19a,21]

Herein, we report that the new 1D coordination polymer [Zn(3-tba)$_2$]·DMA (**1α**; 3-Htba = 3-(4*H*-1,2,4-triazol-4-yl)benzoic acid; DMA = *N*,*N*-dimethylacetamide), **1α**, underwent SCSC transformation to **1β**, a nonporous phase, upon removal of DMA. **1β** in turn transformed to a discrete, binuclear complex, **2**, upon exposure to water vapour. Insight into these reversible transformations comes from the results of SCXRD studies.

Solvothermal reaction of 3-Htba with Zn(NO$_3$)$_2$·6H$_2$O in DMA at 105 °C afforded diamond-shaped crystals of **1α** (synthetic details are available in ESI†). SCXRD revealed that **1α** crystallized in the triclinic space group $P\bar{1}$ and that it displays a 1D chain structure with spiro linkages (Fig. 1). Zn(II) cations adopt a tetrahedral coordination geometry through two oxygen atoms from different 3-tba ligands and two nitrogen atoms from two additional 3-tba ligands. Pairs of 3-tba ligands serve as V-shaped linkers between adjacent Zn(II) cations to form [Zn$_2$(3-tba)$_2$] rings that are further connected into a one-dimensional (1D) coordination polymer (Fig. 1). Adjacent chains are cross-linked by C–H···O interactions (C···O = 3.049(6)–3.097(6) Å, H···O = 2.39–2.44 Å, C–H···O = 127–128°) to form a supramolecular layer (Fig. S1, ESI†). π–π and C–H···π

[a] *Faculty of Chemistry and Chemical Engineering, Yunnan Normal University, Kunming, 650500, China. E-mail: zaxchem@126.com*
[b] *Department of Chemical Sciences, Bernal Institute, University of Limerick, Limerick, V94T9PX, Ireland. E-mail: xtal@ul.ie*

† Electronic supplementary information (ESI) available: Experimental details, single-crystal XRD data, PXRD patterns, IR spectra, TGA curves, *etc.* CCDC 2160142–2160144. For ESI and crystallographic data in CIF or other electronic format see DOI: https://doi.org/10.1039/d2cc02777a

‡ These authors contributed equally to this work.

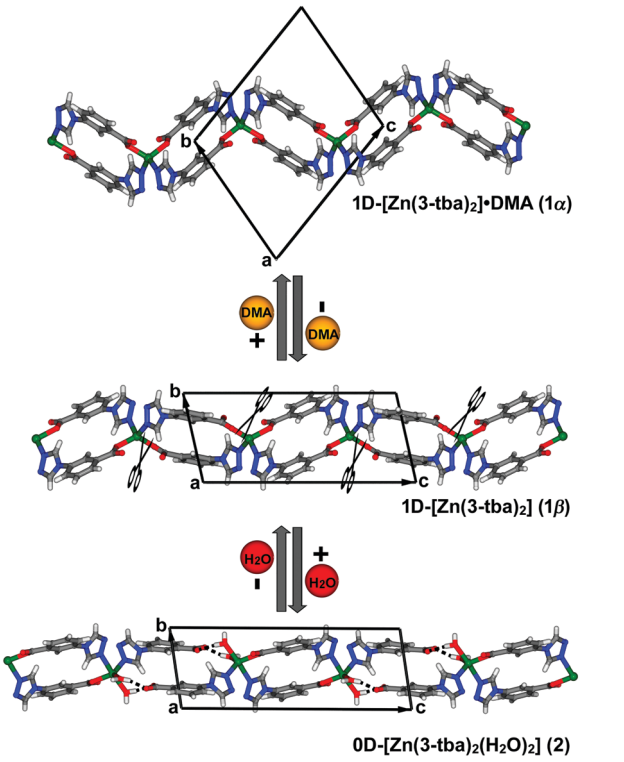

Fig. 1 Structural transformations in $[Zn(3\text{-tba})_2]$ involving **1α**, **1β** and **2** (unit cells are illustrated). Charge-assisted H-bonding (black broken lines) occurs between aqua ligands and free carboxylate moieties in **2**.

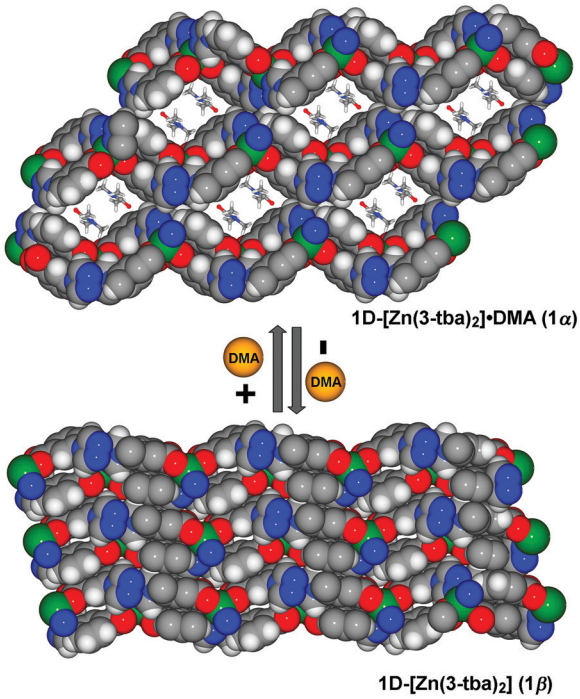

Fig. 2 Space-filing diagrams of the reversible structural transformation between **1α** and **1β** (viewed along the *a*-axis, for more details see Fig. S5, ESI†).

interactions between 1D chains also stabilise the supramolecular layer (Fig. S2, ESI†) which pack through C–H···N interactions (C···N = 3.486(6) Å, H···N = 2.57 Å, C–H···N = 168°) between layers (Fig. S3, ESI†). Along the *a*-axis, the crystal packing of **1α** results in 1D rhombic channels with an effective pore diameter of 4.9 × 7.3 $Å^2$ (Fig. 2 and Fig. S4, ESI†). Void volume in the channel (310.3 $Å^3$) is *ca.* 27.4% of the crystal volume (1134.2 $Å^3$) which is occupied by DMA guest molecules. Thermogravimetric analysis (TGA) revealed that as-synthesized **1α** loses guest molecules (obs. 16.11%, calc. 16.47%) from 78 °C to 180 °C and remains stable to 290 °C (Fig. S17, ESI†).

Heating **1α** under vacuum at 150 °C overnight resulted in SCSC transformation to **1β**. SCXRD revealed that the **1β** is a contorted version of **1α** with the same connectivity. **1β** also crystallized in triclinic space group $P\bar{1}$ but with 24.8% shrinkage of its unit-cell volume relative to **1α**. PLATON calculations indicated that **1β** contains no residual solvent-accessible void and so it is nonporous (Fig. 2). TGA and FT-IR data support the guest-free nature of **1β** (Fig. S17 and S19, ESI†). Transformation between **1α** and **1β** was accompanied by distortions of $[Zn_2(3\text{-tba})_2]$ rings and contraction of interstitial spaces (Fig. S5, ESI†). Meanwhile, rotation of the 3-tba ligand and a hinge-like motion associated with carboxylate coordination occurred (Table S2, ESI†). Aromatic π–π stacking interactions were found to be present in **1β** (Tables S4, S5 and Fig. S7, ESI†). The structural transformation associated with guest removal was found to be reversible as **1β** reverted to **1α** after soaking in DMA at room temperature for 1 day (Fig. 3 and Fig. S9, ESI†). **1β** was observed to transform to a new phase, **2**, after exposure to humidity (Fig. S11 and S12, ESI†).

Single crystals of **2** were obtained after exposure of **1β** to water vapour (vial-in-vial method, details in the ESI†). Such SCSC transformations of low-dimensional coordination networks between multiple phases are relatively rare.[22] SCXRD revealed that the formation of **2**, $[Zn(3\text{-tba})_2(H_2O)_2]$, a discrete complex, involved the following: (a) change from 1-D to 0-D dimensionality; (b) cleavage of some Zn–carboxylate coordination bonds; (c) insertion of coordinated water molecules that form hydrogen bonds to the uncoordinated carboxylate moieties; (d) change of the Zn coordination geometry from tetrahedral to trigonal bipyramidal. As revealed by Fig. 1, **2** is composed of Zn(II) ions that adopt a distorted trigonal bipyramidal coordination geometry (τ = 0.77) with two nitrogen atoms from two 3-tba ligands, one oxygen atom from another 3-tba ligand and two coordinated water molecules. Coordination of water molecules to Zn(II) in effect results in the insertion of water molecules into a Zn–carboxylate bond and formation of charge assisted hydrogen bonds (O···O = 2.535 and 2.626 Å, Fig. 1). Furthermore, the other hydrogen atom from one of the coordinated water molecules formed H-bonds (O···O = 2.737 Å) with uncoordinated O atoms of 3-tba ligands in adjacent complexes whereas the remaining hydrogen atom formed bifurcated H-bonds with two basic N atoms (O···N = 3.146 and 3.254 Å, Fig. S8, ESI†). The FT-IR spectrum of **2** indicates that C=O (1600 cm^{-1}) and C–O (~1051 cm^{-1}) vibrations are different from **1α** and **1β**, consistent with the respective coordination environments (Fig. S19, ESI†). In contrast to **1α** and

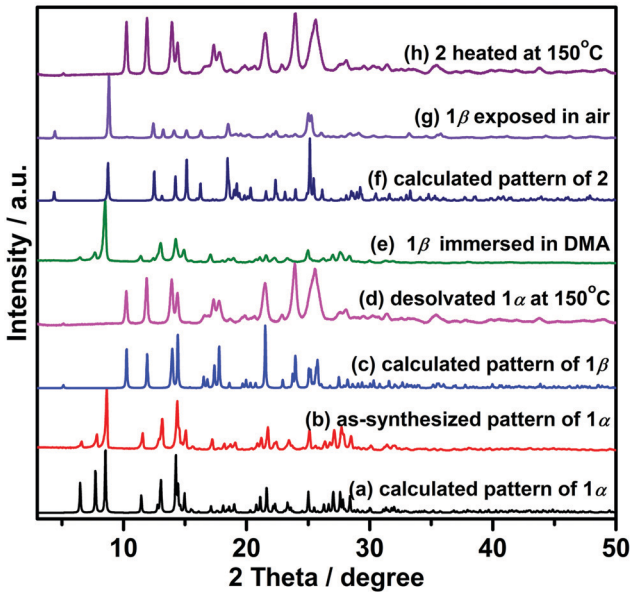

Fig. 3 PXRD patterns of (a) **1α** calculated from SCXRD data, (b) as-synthesized **1α** at room temperature, (c) **1β** calculated from SCXRD data, (d) desolvated **1α** at 150 °C, (e) **1β** immersed in DMA for 1 day, (f) calculated **2** from SCXRD data, (g) **1β** exposed to humid air (*ca.* 45% RH), and (h) dehydrated **2** at 150 °C.

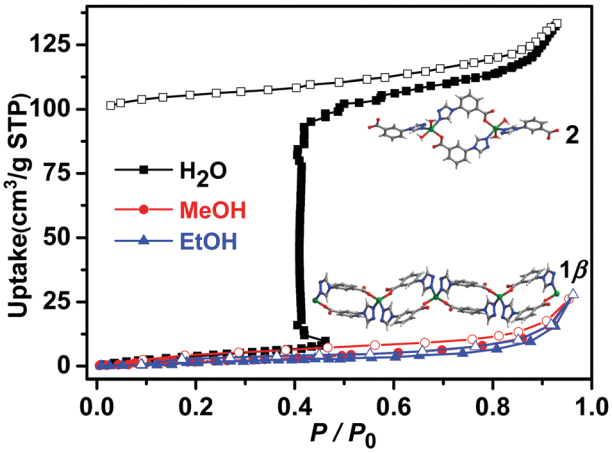

Fig. 4 Water, methanol and ethanol vapour sorption isotherms of **1β** collected at 298 K (closed and open symbols denote adsorption and desorption, respectively).

1β, there are no aromatic π–π stacking interactions between triazole rings (Table. S4, ESI†) but multiple O–H···O and O–H···N hydrogen bonds formed between aqua ligands and uncoordinated N or O atoms of 3-tba ligands (Table S3 and Fig. S8, ESI†). **2** was found to reversibly revert to **1β** *in vacuo* at 150 °C (Fig. S10, ESI†). Attempts to obtain **2** by direct routes were unsuccessful.

Gas sorption experiments for N_2 at 77 K and CO_2 at 195 K were performed on **1β**, which exhibited a type II nitrogen adsorption isotherm (Fig. S20, ESI†) characteristic of a non-porous solid. The BET surface area was determined to be 5.6 $m^2\ g^{-1}$. The CO_2 adsorption isotherm collected at 195 K likewise indicated that **1β** is nonporous (Fig. S13 and S20, ESI†).

Vapour sorption isotherms of water, methanol and ethanol for **1β** were conducted at 298 K. As shown in Fig. 4, no water was adsorbed in the low humidity region but water uptake showed a sudden increase (step) at 46% RH. Such a profile is consistent with a structural transformation. The desorption isotherm exhibits large hysteresis, indicating strong sorbate–water interactions as would be expected from the crystal structure of **2**. To our knowledge, this is the first example of a water-induced 1D → 0D SCSC structural transformation with a one-step type F-IV adsorption isotherm (Table S6, ESI†). At 50% RH, the uptake reached 102 $cm^3\ g^{-1}$, corresponding to approximately 2.0 H_2O molecules per Zn cation, a value in accordance with the TGA measured for **1β** exposed to water vapour for one day (Fig. S18, ESI†). As revealed by Fig. 4, methanol and ethanol adsorption exhibited no uptake up to $P/P_0 = 0.96$. To the best of our knowledge, only one example of a sorbent that displays selective water uptake over alcohols has been observed for materials with type F-IV isotherms.[21a]

In **1β**, one Zn–carboxylate bond in each formula unit deviates from the carboxylate group plane (20.6°, Table S2 and Fig. S5, ESI†). The structure of **2** indicates that two water molecules had in effect inserted into a Zn–carboxylate bond, in turn forming two charge assisted OH···carboxylate H-bonds (Fig. 1). Such a motif has been observed in molecular crystals as exemplified by DL-tartaric acid monohydrate[23] and there are *ca.* 1400 hits in the CSD database for this motif. The coordination of water molecules and charge assisted OH···carboxylate hydrogen bonds supports this water-induced phase transformation. It seems unlikely that the structure of **2** would exist with MeOH or EtOH molecules as there is also H-bonding to the adjacent chains (Fig. S5 and S8, ESI†), perhaps explaining why MeOH and EtOH were not adsorbed.

The sorption isotherms of **1β** for acetonitrile, acetone and benzene also indicated no uptake (Fig. S22, ESI†) and PXRD data revealed that crystals of **1β** were unaffected by exposure to methanol, ethanol, acetonitrile, acetone or benzene vapours in contrast to water vapour, which induced transformation from **1β** to **2** (Fig. S14 and S15, ESI†). Not only was **1β** selective for water, but it was found to retain its water uptake after 5 consecutive activation–uptake cycles (Fig. 5 and Fig. S16, ESI†), indicating that **1β** is recyclable.

In summary, we report a new 1D coordination polymer, $[Zn(3\text{-tba})_2]$ (**1α**), that transformed to **1β** upon removal of guests. **1β** further transformed to a 0D aqua complex $[Zn(3\text{-tba})_2(H_2O)_2]$, **2**, upon exposure to water vapour above 40% RH. Both transformations were verified by SCXRD studies and found to be reversible. Interestingly, **1β** exhibited a one-step type F-IV water adsorption isotherm concomitant with the 1D → 0D SCSC structural transformation. The coordination of two water molecules and self-assembly sustained by charge-assisted OH···carboxylate hydrogen bonds are likely key drivers for this switching event along with other H-bonds formed by the aqua ligands. The water-triggered transformation enabled selective and reversible adsorption of water vapour over other vapours such as methanol, ethanol, acetone, acetonitrile and

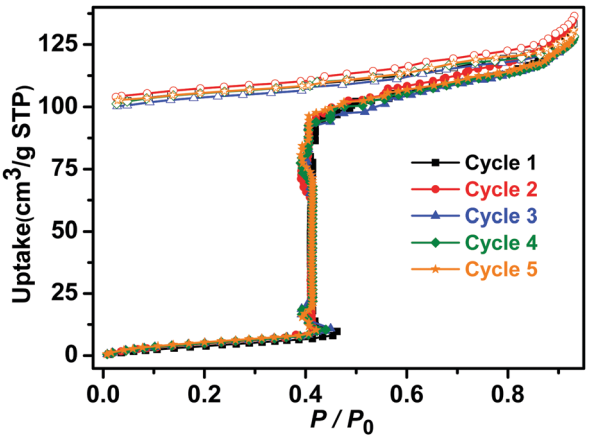

Fig. 5 Five consecutive activation–uptake cycles of water sorption isotherms of **1*β*** at 298 K (closed and open symbols denote adsorption and desorption, respectively).

benzene. Transformation between **1*β*** and **2** implies that there could be other low-dimensional MOMs or molecular compounds that might serve as switching water sorbents given that there are *ca.* 1400 crystal structures with diaqua-carboxylate motifs archived in the CSD.

This work was financially supported by the National Natural Science Foundation of China (No. 22161052) and Science Foundation Ireland (SFI Awards 13/RP/B2549 and 16/IA/4624). S. M. acknowledges an SFI-IRC Pathways award (21/PATH-S/9454) from Science Foundation Ireland.

Conflicts of interest

There are no conflicts to declare.

Notes and references

1 J. J. Perry IV, J. A. Perman and M. J. Zaworotko, *Chem. Soc. Rev.*, 2009, **38**, 1400–1417.
2 L. R. MacGillivray, *Metal-organic frameworks: design and application*, John Wiley & Sons, 2010.
3 (*a*) S. Kitagawa, R. Kitaura and S. Noro, *Angew. Chem., Int. Ed.*, 2004, **43**, 2334–2375; (*b*) S. R. Batten, S. M. Neville and D. R. Turner, *Coordination polymers: design, analysis and application Introduction*, Royal Society of Chemistry; London, 2009.
4 (*a*) J.-R. Li, J. Sculley and H.-C. Zhou, *Chem. Rev.*, 2012, **112**, 869–893; (*b*) X. Han, S. Yang and M. Schröder, *Nat. Rev. Chem.*, 2019, **3**, 108–118; (*c*) S. Mukherjee, A. V. Desai and S. K. Ghosh, *Coord. Chem. Rev.*, 2018, **367**, 82–126; (*d*) Y. Wang, S. B. Peh and D. Zhao, *Small*, 2019, **15**, 1900058; (*e*) T. Wang, E. Lin, Y.-L. Peng, Y. Chen, P. Cheng and Z. Zhang, *Coord. Chem. Rev.*, 2020, **423**, 213485.
5 P. Z. Moghadam, A. Li, X.-W. Liu, R. Bueno-Perez, S.-D. Wang, S. B. Wiggin, P. A. Wood and D. Fairen-Jimenez, *Chem. Sci.*, 2020, **11**, 8373–8387.
6 (*a*) S.-Q. Wang, S. Mukherjee and M. J. Zaworotko, *Faraday Discuss.*, 2021, **231**, 9–50; (*b*) Q.-Y. Yang, P. Lama, S. Sen, M. Lusi, K.-J. Chen, W. Y. Gao, M. Shivanna, T. Pham, N. Hosono, S. Kusaka, J. Perry IV, S. Ma, B. Space, L. J. Barbour, S. Kitagawa and M. Zaworotko, *Angew. Chem., Int. Ed.*, 2018, **57**, 5684–5689.
7 J. A. Mason, J. Oktawiec, M. K. Taylor, M. R. Hudson, J. Rodriguez, J. E. Bachman, M. I. Gonzalez, A. Cervellino, A. Guagliardi, C. M. Brown, P. L. Llewellyn, N. Masciocchi and J. R. Long, *Nature*, 2015, **527**, 357–361.
8 (*a*) N. Nijem, H. Wu, P. Canepa, A. Marti, K. J. Balkus Jr., T. Thonhauser, J. Li and Y. J. Chabal, *J. Am. Chem. Soc.*, 2012, **134**, 15201–15204; (*b*) M. L. Foo, R. Matsuda, Y. Hijikata, R. Krishna, H. Sato, S. Horike, A. Hori, J. Duan, Y. Sato, Y. Kubota, M. Takata and S. Kitagawa, *J. Am. Chem. Soc.*, 2016, **138**, 3022–3030; (*c*) M. K. Taylor, T. Runčevski, J. Oktawiec, J. E. Bachman, R. L. Siegelman, H. Jiang, J. A. Mason, J. D. Tarver and J. R. Long, *J. Am. Chem. Soc.*, 2018, **140**, 10324–10331.
9 M. Shivanna, K.-i Otake, B.-Q. Song, L. M. van Wyk, Q.-Y. Yang, N. Kumar, W. K. Feldmann, T. Pham, S. Suepaul, B. Space, L. J. Barbour, S. Kitagawa and M. J. Zaworotko, *Angew. Chem., Int. Ed.*, 2021, **133**, 20546–20553.
10 (*a*) G. K. Kole and J. J. Vittal, *Chem. Soc. Rev.*, 2013, **42**, 1755–1775; (*b*) J.-P. Zhang, P.-Q. Liao, H.-L. Zhou, R.-B. Lin and X.-M. Chen, *Chem. Soc. Rev.*, 2014, **43**, 5789–5814.
11 (*a*) S. Horike, S. Shimomura and S. Kitagawa, *Nat. Chem.*, 2009, **1**, 695–704; (*b*) E. Fernandez-Bartolome, A. Martinez-Martinez, E. Resines-Urien, L. Piñeiro-Lopez and J. S. Costa, *Coord. Chem. Rev.*, 2022, **452**, 214281.
12 (*a*) J. Liu, X.-P. Zhang, T. Wu, B.-B. Ma, T.-W. Wang, C.-H. Li, Y.-Z. Li and X.-Z. You, *Inorg. Chem.*, 2012, **51**, 8649–8651; (*b*) S. Sen, S. Neogi, K. Rissanen and P. K. Bharadwaj, *Chem. Commun.*, 2015, **51**, 3173–3176.
13 (*a*) Z. Xie, L. Mei, Q. Wu, K. Hu, L. Xia, Z. Chai and W. Shi, *Dalton Trans.*, 2017, **46**, 7392–7396; (*b*) S. M. Mobin, A. K. Srivastava, P. Mathur and G. K. Lahiri, *Dalton Trans.*, 2010, **39**, 8698–8705.
14 H.-C. Fang, J.-Q. Zhu, L.-J. Zhou, H.-Y. Jia, S.-S. Li, X. Gong, S.-B. Li, Y.-P. Cai, P. K. Thallapally, J. Liu and G. J. Exarhos, *Cryst. Growth Des.*, 2010, **10**(7), 3277–3284.
15 (*a*) J.-M. Chen, Y.-X. Hou, Q.-K. Zhou, H. Zhang and D. Liu, *Dalton Trans.*, 2017, **46**, 9755–9759; (*b*) R. Medishetty, A. Husain, Z. Bai, T. Runčevski, R. E. Dinnebier, P. Naumov and J. J. Vittal, *Angew. Chem., Int. Ed.*, 2014, **53**, 5907–5911.
16 (*a*) C. K. Brozek and M. Dincă, *Chem. Soc. Rev.*, 2014, **43**, 5456–5467; (*b*) E. Papazoi, A. Douvali, S. Rapti, E. Skliri, G. S. Armatas, G. S. Papaefstathiou, X. Wang, Z.-F. Huang, S. Kaziannis, C. Kosmidis, A. G. Hatzidimitriou, T. Lazarides and M. J. Manos, *Inorg. Chem. Front.*, 2017, **4**, 530–536.
17 (*a*) J.-Y. Wu, Y.-C. Liu and T.-C. Chao, *Inorg. Chem.*, 2014, **53**, 5581–5588; (*b*) J. Fu, H. Li, Y. Mu, H. Hou and Y. Fan, *Chem. Commun.*, 2011, **47**, 5271–5273.
18 S.-Y. Ke and C.-C. Wang, *CrystEngComm*, 2015, **17**, 8776–8785.
19 (*a*) S. K. Ghosh, W. Kaneko, D. Kiriya, M. Ohba and S. Kitagawa, *Angew. Chem., Int. Ed.*, 2008, **47**, 8843–8847; (*b*) J. Albalad, J. Arinez-Soriano, J. Vidal-Gancedo, V. Lloveras, J. Juanhuix, I. Imaz, N. Aliaga-Alcaldebd and D. Maspoch, *Chem. Commun.*, 2016, **52**, 13397–13400; (*c*) W.-B. Chen, Y.-C. Chen, M. Yang, M.-L. Tong and W. Dong, *Dalton Trans.*, 2018, **47**, 4307–4314.
20 (*a*) N. C. Burtch, H. Jasuja and K. S. Walton, *Chem. Rev.*, 2014, **114**, 10575–10612; (*b*) J. Canivet, A. Fateeva, Y. Guo, B. Coasne and D. Farrusseng, *Chem. Soc. Rev.*, 2014, **43**, 5594–5617; (*c*) M. J. Kalmutzki, C. S. Diercks and O. M. Yaghi, *Adv. Mater.*, 2018, **30**, 1704304.
21 (*a*) S. K. Ghosh, J.-P. Zhang and S. Kitagawa, *Angew. Chem., Int. Ed.*, 2007, **46**, 7965–7968; (*b*) A. K. Gupta, S. S. Nagarkar and R. Boomishankar, *Dalton Trans.*, 2013, **42**, 10964–10970; (*c*) S. S. Nagarkar and S. K. Ghosh, *J. Chem. Sci.*, 2015, **127**, 627–633.
22 (*a*) A. Kondo, T. Nakagawa, H. Kajiro, A. Chinen, Y. Hattori, F. Okino, T. Ohba, K. Kaneko and H. Kanoh, *Inorg. Chem.*, 2010, **49**, 9247–9252; (*b*) A. V. Gavrikov, A. B. Ilyukhin and P. S. Koroteev, *CrystEngComm*, 2020, **22**, 2895–2899; (*c*) W.-B. Chen, Y.-C. Chen, G.-Z. Huang, J.-L. Liu, J.-H. Jia and M.-L. Tong, *Chem. Commun.*, 2018, **54**, 10886–10889; (*d*) C. D. Ene, C. Maxim, M. Rouzières, R. Clérac, N. Avarvari and M. Andruh, *Chem. – Eur. J.*, 2018, **24**, 8569–8576.
23 T. Fukami, S. Tahara, C. Yasuda and K. Nakasone, *Int. J. Chem.*, 2016, **8**, 9–21.